Ferroelectric Properties of Terbium Doped Multiferroics

Hage Doley[1,*], P.K.Swain[2], Hu Xinghao[3,] Upendra Singh[4]

[1]Dera Natung Govt. College, Itanagar 791113, India

[2]National Institute of Technology, Jote 791119, India

[3]Institute of Intelligent Flexible Mechatronics, Jiangsu University, Zhenjiang, PR China

[4]Department of computer science and engineering, Graphic Era Deemed to be University, Dehradun, India

Email: hagedoley@dngc.ac.in

Abstract

Solid Solution of (1-x)$Ba_5TbTi_3V_7O_{30}$-x$BiFeO_3$ is fabricated using Solid State Reaction technique for various x values. Single-phase compound formation is confirmed by the XRD (X-Ray Diffractogram). Using Scanning Electron Microscope (SEM: JOEL-IT300) grain morphology is analysed. It can be seen that with an increase in x, the average grain size also increases. Ferroelectric characteristics such as Dielectric constant and loss tangent at temperature range (Room Temp – 500℃) and various frequencies range are measured by Impedance Analyser (HIOKI-IM3536). Samples were found to be ferroelectric in nature and with an increase in $BiFeO_3$ content, the dielectric constant decreases.

Keywords. Dielectric Constant, Ferroelectric, Loss Tangent, Multiferroic.

7.1. INTRODUCTION

Due to various applications of ceramic materials, ceramic processing plays a vital role in modern technology. Ferroelectric ceramic is the kind of such ceramic compound which have been extensively studied.

Ferroelectric is a special type of dielectrics. Broadly, crystalline dielectrics are of two types: (a) Polar and (b) Non-Polar. Polar dielectric has dipole moments even when there is no external field whereas there is no such dipole moment in the case of Non-Polar dielectric. In the case of Polar dielectric, the polarization appears due to the unit cell's inherent symmetry, giving rise to electronic/ionic polarization and creating a dipole moment. Thus, ferroelectric materials have spontaneous polarization which could be reversed by applying a reverse electric field. The polarization reversal of dielectric was

first observed by Valasek in 1920 [1]. The non-linear relation of polarization with the electric field is one of the main features of ferroelectrics [2-5]. Nye [6] and Bhagavantam [7] discussed the effect of symmetry on the properties of the crystal. There are in total 32 possible point groups based on crystal symmetry elements. For a material to show ferroelectric properties it should lack a centre of symmetry (necessity but not sufficient condition). There are 21 classes and 32-point groups that lack a centre of symmetry of which 20 crystal classes could be polarized under external stress and such type of material is called piezoelectric materials. 10 out of such piezoelectric groups also show pyroelectric behaviour. As the temperature changes, polarization is observed in the form of a pyroelectric current. Ferroelectrics are a subgroup of pyroelectric in which polarization could be reoriented or reversed by applying a reverse external field. A typical ferroelectric has spontaneous polarization which decreases with temperature and disappears at a particular temperature is known as Curie temperature (T_C) [8]. At which material undergo a transition from ferroelectrics to paraelectric phase. The paraelectric phase is more symmetric than the corresponding ferroelectric phase. The dielectric constant above the transition temperature is also called Curie temperature (T_C) obeys the Curie-Weiss law [9]:

$$\varepsilon = \varepsilon_0 + \frac{C}{T - T_C} \tag{7.1}$$

7.1.1. Classification of Ferroelectrics

All the known ferroelectrics today can conveniently be classified into 4 main groups based on their chemical compositions and structures. 1. Rochelle salt ($NaKC_4H_4O_6.4H_2O$) [1]. It is the representative of the tartrate group. 2. KDP (KH_2PO_4) [10]. This is a typical example of the dihydrogen phosphate of alkali metal. 3. Oxygen octahedra group which could again be subdivided into two main groups. Perovskite and tungsten-bronze (TB) structure. The general formula for perovskite is ABO_3 [3] and for TB it is $[A1_2A2_4C_4][B1_2B2_8]O_{30}$. 4. $NHC(NH_2)2AlH(SO_4)_2.6H_2O$ (Guanidine aluminium sulphate hexahydrate) [11]. As the present work concerns with the TB type compounds, we give detailed information about them:

- Oxygen octahedral crystal is one of the most essential groups in the family of ferroelectrics. It has a structure having a combination of oxygen octahedra (located at the centre) and voids (occupied by other ions).
- The oxygen octahedra ferroelectric family has three possible basic structures: (1) Perovskite (2) Trigonal Ilmenite structure (3) Distorted potassium- TB structure.

The basic octahedral framework of the TB structure could be seen in Figure 7.1. The tetragonal unit cell consists of 10 BO_6 octahedra connected in such a way forming three different kinds of tunnels passing parallel to the c-axis. Its unit cell has a height of about 4nm (one octahedron) along the c-axis direction along with $a = b$ dimension of about 1.25nm ($\sim\sqrt{10}c$). The long oxygen octahedra chains along the c-axis bear a resemblance to the perovskite structure whereas normal to this axis consists of slightly

puckered oxygen atoms sheets. Depending on the type of composition A-type cations could enter the interstitial tunnels in various ways. Such arrangements give space for about 4 (four) cations in 15 co-radiated trigonal A2 sites and 2 (two) cations in smaller 12 (twelve) co-ordinated planar C-sites as can be seen from the figure. In addition to that, there are also two different B cation sites called B1 and B2.

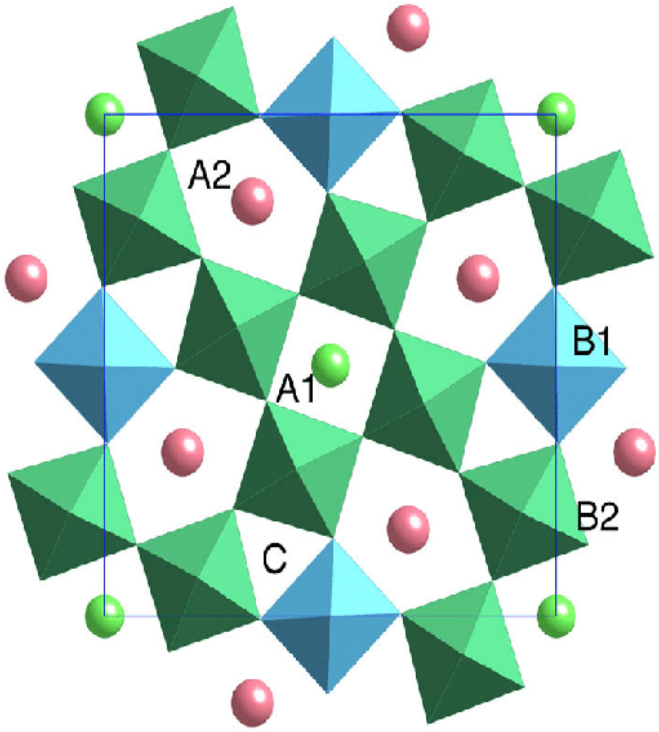

Figure 7.1. The atomic arrangement of a unit cell TB- type structure.

The TB structure may be categorized in the following general formula:

$$(A1)_x(A2)_{5-x}Nb_{10}O_{30}$$

- $(A1)_x(A2)_{5-x}Nb_{10}O_{30}$, where A1 and A2 are alkaline earth ions. The best-known and most widely studied compound is $Sr_{5x}Ba_xNb_{10}O_{30}$. In this, the unit cell has five formula units and five alkaline earth cations which could fill the six interstitials A1 and A2 sites Both Sr and Ba ions are too large to enter the c-sites. The structures are not filled, and a certain degree of randomness can be seen.
- $(A1)_x(A2)_{2-2x}Nb_{10}O_{30}$, where A1 is an alkaline earth and A2 is an alkali ion. For example – $Ba_{4+x}Na_{2-2x}Nb_{10}O_{30}$ (BNN). Here, A1, A2 sites are filled, and C site is empty. This is also called a filled structure.
- $(A1)_{6-x}(A2)_{4+x}Nb_{10}O_{30}$, where A1 and A2 are alkali ions. For example, $K_{6-x}Li_{4+x}Nb_{10}O_{30}$ (KLN), Here all A1, A2 and C sites are expected to be all

filled up along with smaller Li-ion in the C-site. In all the above types, properties depend on the width of x of solid solution regions.

7.1.2. Multiferroic and their importance

Multiferroic materials are getting much importance in recent years for it presents both ferromagnetism and ferroelectricity properties in the same material. They could have utility in designing a new type of RAM where both the electric and magnetic polarisation could be used for storing data. Apart from the multiferroic composites processing [12] and thin films, the look for bulk multiferroic is a pressing challenge.

Multiferroic materials can explore magnetic states by modulating an electric field and vice versa. It has lots of potential utilities such as storing information in sensors and spintronic devices [13]. However, there exists very few single-phase multiferroics in normal temperatures. It is due to the unsustainability [14] of conventional mechanisms, cations are off-centre in ferroelectrics which require empty d orbitals whereas magnetic moment requires partially filled d orbitals. For the coexistence of ferroelectrics and magnetic properties in a single phase, the ions should be off-centre to form an electric dipole moment which is of a different mechanism than that of a magnetic moment. In the ABO_3 type (magnetic perovskite-type structure oxides), the multiferroic property is due to the stereochemical activity of lone pair of large cations (A-type) which provides ferroelectric property whereas, the B-type cation provides magnetic moment. In this regard, Bi-based magnetic ferroelectrics like Bismuth Ferrite ($BiFeO_3$) draw huge attention in recent years. It has both the ferroelectric and antiferromagnetic order in the same phase at room temperature. In this material, there also exists magnetoelectric coupling between spin and charge. In $BiFeO_3$, Fe^{3+} ions are magnetic whereas Bi ion having lone pair (two electrons) in 6s orbital moves away from a centre centrosymmetric position of oxygen surrounding resulting into ferroelectric properties. $BiFeO_3$ has a structure of non-centrosymmetric rhombohedral distorted perovskite structure.

Various types of multiferroic have been studied but $BiFeO_3$ has been able to derive the most attention due to the simultaneous existence of ferroelectric order having Curie temperature (Tc~ 1083K) and antiferromagnetic order having Neel point (T_N ~ 625K). Till now, only Bismuth ferrite $BiFeO_3$ has been able to show multiferroic behaviour at normal temperature; however, its complex antiferromagnetic order yields only a tiny remnant magnetization [15]. At room temperature, $BiFeO_3$ has the potential for many magnetoelectric applications. It also could have applications such as switches, actuators, electronic memory devices, magnetic sensors, etc.

Due to the low value of the dielectric constant and its superstructure, earlier it was believed that $BiFeO_3$ is antiferroelectric in nature. However, Tabares- Munoz et al. [16] using a polarized light microscope observed the ferroelectricity and ferroelasticity in $BiFeO_3$ thus confirming the ferroelectric nature of the material. However, it is very difficult to observe the ferroelectric loop at room temperature due to its low resistivity at room temperature. Teague *et al.* [17] increased its resistivity by observing and measuring the hysteresis loop at low temperatures i.e., 80K. It was found that materials

have ferroelectric properties along with ferroelastic properties and antiferromagnetic properties. Since it shows both ferroelectric and magnetic properties it is also known as magnetoelectric material. At room temperature, due to the semiconducting nature of Bismuth Ferrite electrical poling is difficult because of which it has loss characteristics (i.e., high tangent loss) [18]. To overcome the loss characteristics at high temperatures Smolenskiĭ et al. [19] measured the dielectric constant(ε) in a microwave frequency range. Smith et al. [20] doped the Bismuth Ferrite with other perovskites to enhance the insulator properties. They fabricated $BiFeO_3$-$PbTiO_3$ solid solution having high resistivity, which results in high dielectric along with low loss.

Various kinds of research have been done by mixing $BiFeO_3$ along with other perovskites ABO_3 type to form a solid solution. It was found that $BiFeO_3$ shows different structure transformations along with an increase in secondary phases also.

Mahesh et al [21] established an experimental set-up through which the magnetoelectric effect could be measured. An impedance study was done on solid solution $BiFeO_3 - BaTiO_3$[22]. It was found that there is an increase in lattice parameters due to the doping of $BaTiO_3$ having a tetragonal structure, there is also an increase in conductivity of the system along with a decrease in the transition temperature in comparison to the $BiFeO_3$ thus the sample is showing Debye like behaviour. Further study of $BiFeO_3 - BaTiO_3$[23] reveals that the system undergoes structural modification as the content of $BaTiO_3$ is increased in the system. At the cubic phase, no ferroelectric phase was observed.

Bismuth Ferrite belongs to a displacive type of ferroelectrics, and the structure determines the property of grain and grain boundaries. The antiferromagnetic ordering of $BiFeO_3$ is due to the interactions Fe-O-Fe chain and due to distortion of perovskite structure and canting of spin a weak ferromagnetic property is observed. As the content of the $BaTiO_3$ increases the structure becomes simpler and the paramagnetism sets in. Zhu [24] studied the electrical properties of chemically modified $0.67BiFeO_3 - 0.33BaTiO_3$ferroelectrics solid solution and concluded that chemically modified material has improved dielectric properties and it could have applications as magneto-electric and piezoelectric materials. A study on solid solution $(1-x)BiFeO_3 - xPbTiO_3$multiferroic [25] shows that the system has morphotropic phase boundary with three regions i.e., orthorhombic, rhombohedral, and tetragonal phase co-exist and have three antiferromagnetic order anomalies concerning three stated phases. Nalwa et al [26] doped Sm on $BiFeO_3$ and found that the solid-state reaction of Fe_2O_3 and Bi_2O_3 though does not eliminate the Bi-rich impurity phase; but it is possible to obtain a single phase of Sm doped Bismuth Ferrite having calcination temperature above 1073K; along with an increase in magnetization in magnitude by an order of about two and having Neel temp ~603K. Hence Sm doped $BiFeO_3$ enhances not only remnant polarization but also the conductivity. S. Chandarak et al [27] studied the dielectric characteristics of $(1-x)BiFeO_3 - xPbTiO_3$ and found that the dielectric properties of the ceramics enhanced with an increase of $BaTiO_3$ content; the high dielectric constant is due to the giant- dielectric like behaviour which is due to the Fe multivalent state

along with better grain packing density as the content of $BaTiO_3$ increases in the system. Ceramic $BiFeO_3$- $BaTiO_3$ also has giant-like behaviour similar to that of $BiFeO_3$.

The family of TTB (Tetragonal Tungsten Bronze) structure has lots of advantages over the Perovskites structure. i.e., it has 5 cation sites whereas Perovskites have about 2 sites, the higher number of sites could result in more magnetic interactions. Also, it has a more polar state [28, 29] which could result in the better coupling of ferroelectric and magnetization.

In the TB structure family, Niobates are of great importance. Materials like $Ba_2NaNb_5O_{15}$ or Barium Sodium Niobate (BNN) are among the best ferroelectric materials in the TB structure family [30-32]. Detail structural study was done by Sati et al [33] by doping with different rare earth elements in the BNN. Subsequently, Panigrahi et al developed ferroelectric material $Ba_5RTi_3Nb_7O_{30}$ (R= rare earth elements) [34-35] and studied structural and electrical properties. It was found that the compound is orthorhombic in structure and has diffuse phase transition and change of R we get different Curie temperatures [36].

There are diverse types of ferroelectrics having TB structure [37], among which Niobates are special because of their various utility in the fields of electro-optic, acoustic optic, nonlinear optic, etc. Among which lead containing Niobates such as $(Pb\text{-}Ba)Nb_2O_6$, $PbNb_2O_6$, etc [38, 39] even though has many applications in the field of piezoelectric, pyroelectric, capacitor, etc. But its by-product i.e., Lead oxides are found to be health hazardous. So, there was in need to make Niobates Lead free. The discovery of $(Ba\text{-}Sr)Nb_2O_6$ (BNN) [40, 41] became an important milestone for it's not only free of any lead but also has improved electro-optic coefficient along with diffused phase transitions. After which lots of research are being done in particular material and lot many new materials are also being developed in the same line. And one such kind is the Rare Earth doped Niobate-Titanate (TB structure) material i.e., $Ba_5RTi_3Nb_7O_{30}$ [34,35], having various rare earth element (R) substitutions. But it has high calcination and sintering temperature [42]. However, in $Ba_5RTi_3Nb_7O_{30}$, when Niobium (Nb) is substituted by Vanadium (V) element, then calcination temperature and sintering temperature were found to be reduced [43-45] along with improved thermal stability, low current leakage [46] with enhanced dielectric properties thus better ferroelectric [47,48].

Literature survey shows that the ferroelectric characteristics could be increased when the ferroelectrics are doped with multiferroics such as $BiFeO_3$ [49]. Different materials are being prepared and researched by mixing $BiFeO_3$ (having perovskite structure) with ferroelectrics materials having similar structural family i.e., perovskite structure [45, 50] but in our work we are mixing $BiFeO_3$ with $Ba_5TbTi_3V_7O_{30}$ having different structural (i.e. TB-structure). The reason for the choice of TB structure is that it has a more open structure in comparison to perovskite, which could allow extensive substitution of anion and cation ions ensuring better ferroelectric characteristics as a result, improved magnetic and electric properties thus a better multiferroic.

7.2. MATERIALS AND METHODS

Ferroelectric ceramics have the benefit over single crystal preparation for it is easier and cheaper to fabricate [51]. The composition and structure of phases are not the only determining factors of the ceramic product's properties but also depend on how the phases are being arranged [52]. We have adopted mixed-oxides processes or high-temperature solid-state reaction processes. It is a conventional method that includes the following steps of operation (1) Weighing and mixing (2) pre-firing or calcination (3) grinding (4) sintering. Flow charts depicting the various steps are shown in Figure 7.2. Polycrystalline $Ba_5TbTi_3V_7O_{30}$ were fabricated using a solid-state reaction technique by using raw material of high purity (> 99.9%) carbonates and oxides; $BaCO_3$, V_2O_5, TiO_2, Tb_2O_3 (all from Lobachemie). The required weight of the elements for the fabrication of essential compounds is calculated from the Stoichiometric equation as given:

$$5BaCO_3 + \frac{1}{2}Tb_2O_3 + 3TiO_2 + \frac{7}{2}V_2O_5 = Ba_5TbTi_3V_7O_{30} + 5CO_2$$

The components are weighed using electronic balance maintaining a Stoichiometric ratio, it is then mixed and ground by adding methyl acetate using agate mortar for about 10 hours. The system is then dried through slow evaporation. The powder is then calcined in a muffle furnace using an alumina crucible boat and then using XRD, formation of the sample is confirmed by studying the profile of the powder. After several repeated processes of grinding and calcination at different temperatures and time duration an optimal parameter is established. It was found that for our sample the established parameter is 750℃ heating for about 12 hours. The calcined process powder has a certain degree of pebbles in it due to which it again needs to be crushed to form fine powder using an agate mortar and pestle for about 6 hours and mixed with PVB (Polyvinyl Butyral) as a binding agent. It is then die-pressed using a hydraulic press to apply ~ 7 tons of uniaxial pressure to form a pellet having dimensions of ~13mm diameter and ~2mm thickness. Finally, the processed pellet is sintered at 800℃ for about 12 hours. In the high sintering temperature, all the binding solution gets burned out. The sample is then left cool to room temperature inside the furnace.

Precursor compound of high purity (> 99.9%) oxides: Fe_2O_3 (Lobachemie) and Bi_2O_3 (Lobachemie) are mixed stoichiometrically and calcined at ~700℃ for ~5 h to form Bismuth Ferrite ($BiFeO_3$).

Using the solid-state reaction technique, a solid solution of $(1-x)Ba_5TbTi_3V_7O_{30} - (x)BiFeO_3$ ($x = 0, 0.3, 0.5, 0.7, 1$) is fabricated. The precursor material is then mixed at the proper ratio and calcined at ~ 750 ℃ (at the rate of ~ 1°/min) for about 12 h. A small amount of binder (Polyvinyl Butyral) is put into the processed powder and then using a die, a pressure of ~ 6 tons is applied to prepare a pellet having dimensions of thickness of ~2 mm and diameter of ~13 mm. Pellets are then sintered at ~ 800℃ for about 6 h and cooled by ~ 2°/min. Crystalline phase formation is then established by X-ray diffractogram (Rigaku, Miniflex) having CuKα radiation wavelength of 1.5405 Å within Bragg's angles 2θ (10°< θ< 60°) range having scanning rate 3°/min. The

morphology of the surface is studied using SEM: JOEL-IT300 by polishing an electrode on both sides by applying the silver paste on sintered pallets. Dielectric properties are analyzed using HIOKI-IM3536.

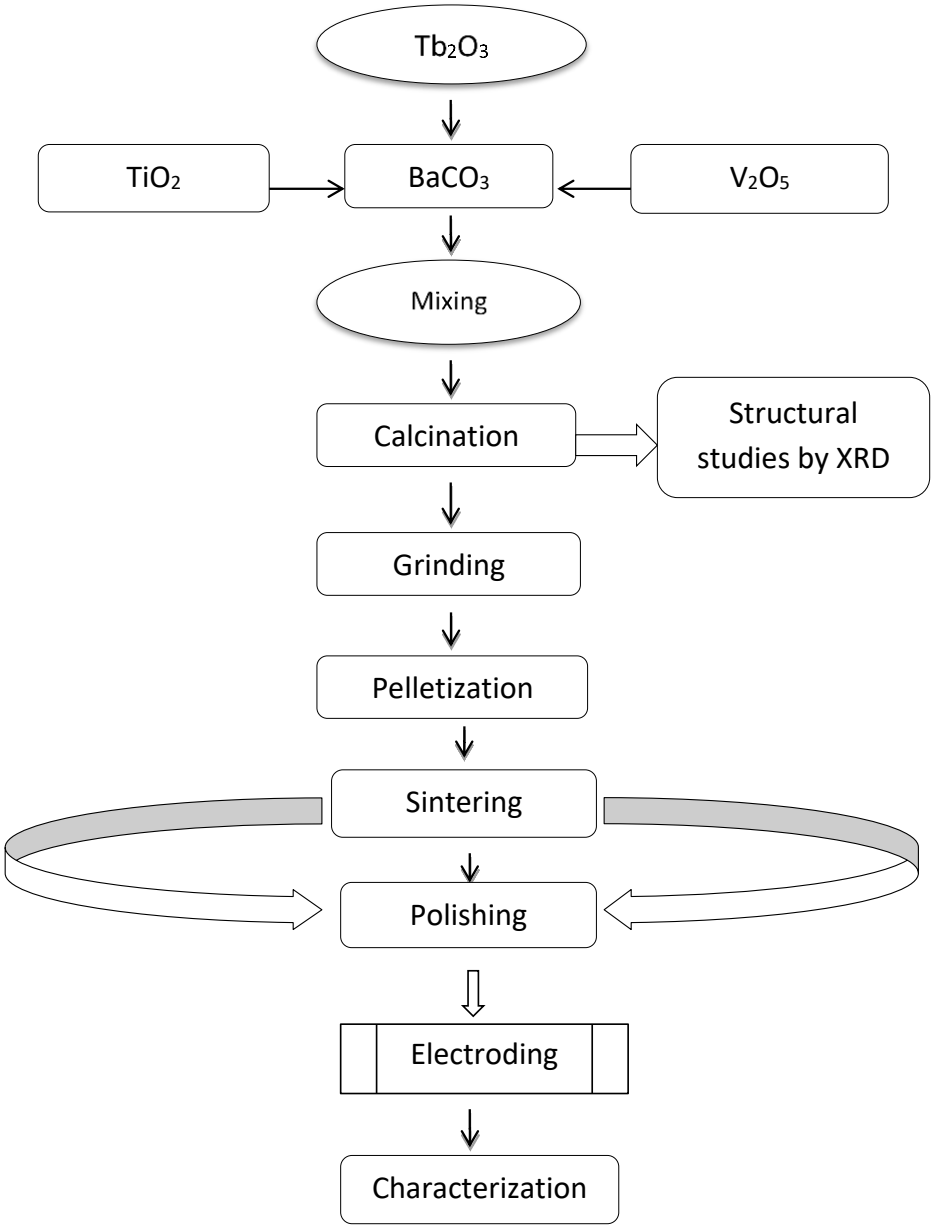

Figure7.2. Flow chart for fabrication of ceramics samples.

7.3. RESULT AND DISCUSSION

7.3.1. Structural studies

The atomic arrangements determine the physical characteristics of solids. Therefore, the crystal structure has a vital role in establishing the classification of a sample. A crystal comprise of small fragments regions in randomness is called poly-crystalline material. The X-ray diffraction technique is an effective method that is not only useful for single crystals but also often used to identify polycrystalline materials. Here the random orientation of crystalline allows a certain fraction of the sample to be suitably oriented along with the axis of the incident beam requisite for producing diffraction phenomena. X-ray diffraction technique based on monochromatic radiation is widely used for determining the atomic spacing from the observed diffraction angles. For the determination of the structure of the specimen, the powder technique in conjunction with a diffractometer is commonly used.

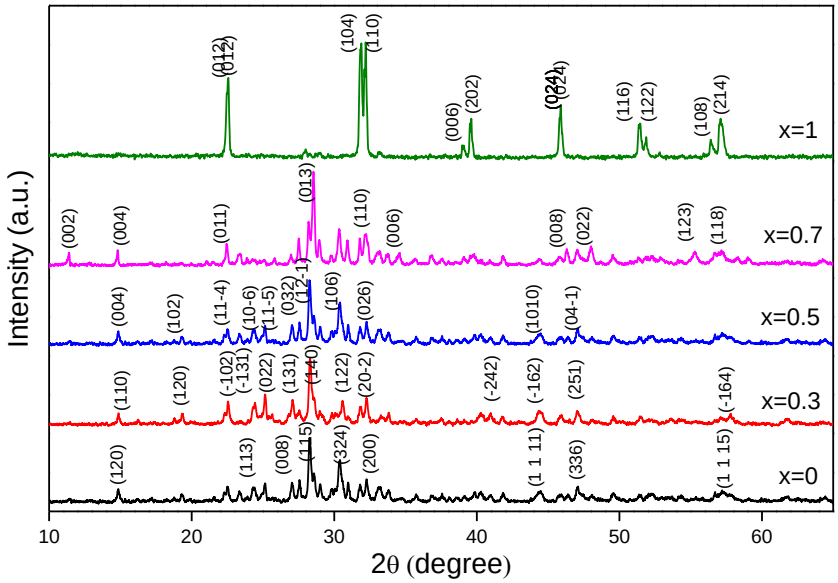

Figure 7.3. XRD pattern for $(1-x)Ba_5TbTi_3V_7O_{30} - (x)BiFeO_3$.

In our experiment, an X-ray diffractometer (Rigaku Miniflex, Japan) was employed in which the specimen is placed at the centre of the diffractometer and then rotated by an angle θ along the axis of the specimen plane. The X-ray source uses CuKα radiation (λ = 1.5418 Å). The counter is attached to the arm rotating along the same axis by 2θ angle (twice to that specimen rotation angle). The focusing circle diameter shrinks continuously as the diffraction angle increases. The (h k l) plane parallel to the specimen plane only contributes to the diffraction pattern and the corresponding d-values (interplanar space) are calculated. The diffractogram investigation is very useful in determining the structure. It can also be used for some of the other problems like phase equilibrium study, chemical analysis, stress measurement, particle size

determination etc. The structural characterization is done by X-ray Diffractometer (XRD) on the calcined powder. From Figure 7.3 it can be seen that at the expected regions there is a single and sharp diffraction peak which confirms that the compound is in a single phase.

7.3.2. Microstructural studies

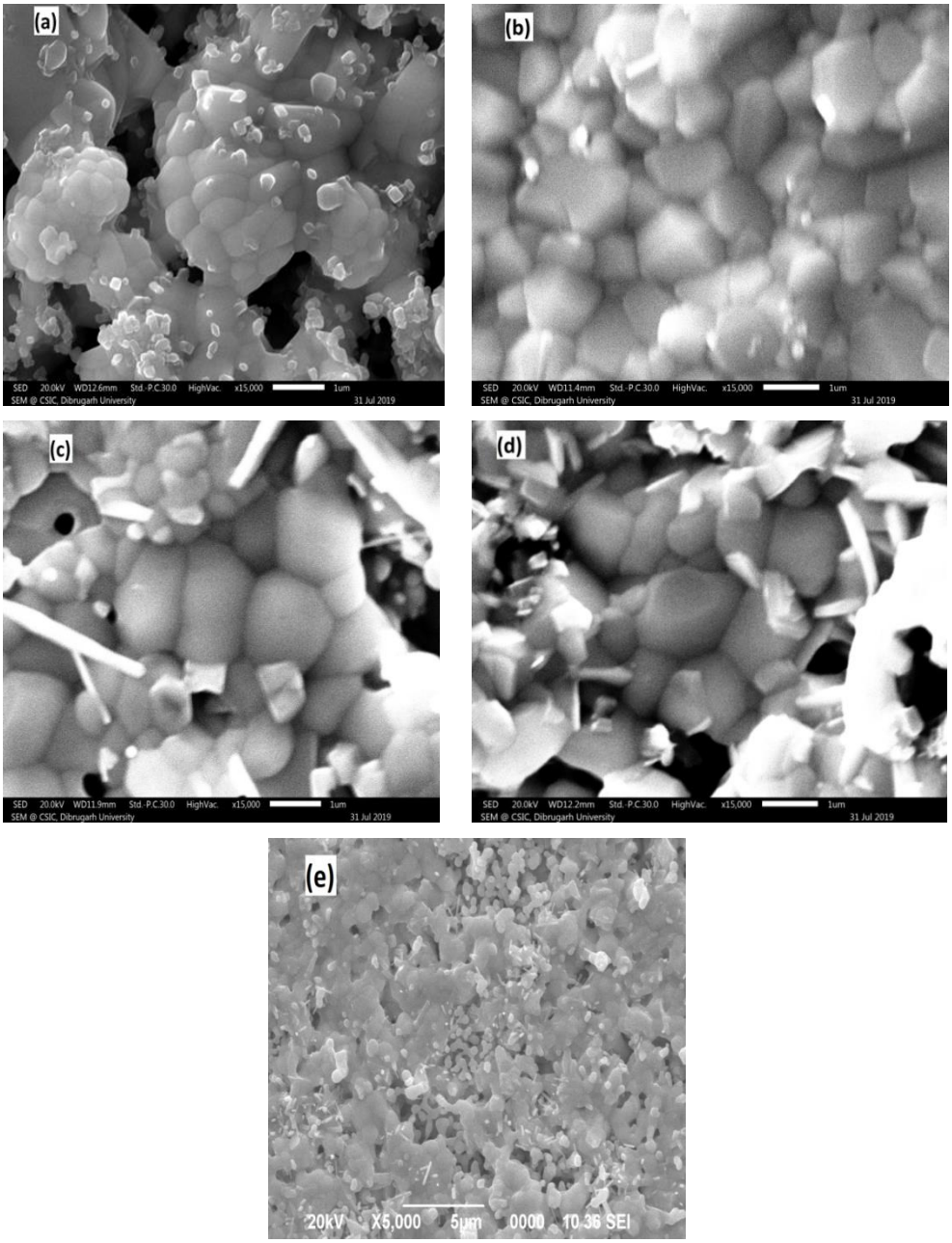

Figure7.4. Micrograph SEM image of $(1-x)Ba_5TbTi_3V_7O_{30} - (x)BiFeO_3$ (a) $x = 0.0$ (b) x =0.3 (c) $x = 0.5$ (d) $x = 0.7$ (e) x =1.

SEM micrographs of $(1-x)Ba_5TbTi_3V_7O_{30} - (x)BiFeO_3$ can be seen in Figure7.4 (a-e). The growth of the grain is almost completed. Using a linear intercept method, the grain size is measured. From the SEM micrograph for $x = 0$ (*i.e.*,$Ba_5TbTi_3V_7O_{30}$) the average size of the grain is about ~0.9 μm. It can also be seen that the granule is elongated, angular and cuboid in shape. There is no secondary recrystallization and the occurrence of voids having irregular dimensions suggests the sample has some degree of porosity and inhomogeneity. From the SEM micrograph for $x = 0.3$ (*i.e.*,$0.7Ba_5TbTi_3V_7O_{30} - 0.3BiFeO_3$) the average size of the grain is about ~1.1μm. With an increase in x, the compactness of the grain also increases and is most compact for $x = 0.3$ and there is an increase in grain size. The distribution of grains is almost homogeneous, and some are spherical in shape. No secondary recrystallization is observed and with the addition of $BiFeO_3$ there is a decrease in the presence of voids. From the SEM micrograph for $x = 0.5$ (*i.e.*, $0.5Ba_5TbTi_3V_7O_{30} - 0.5BiFeO_3$) the average size of the grain is about ~1.9μm. Few columnar and some spherical-shaped grains having inter-grain and intra- grain porosity are also being observed and grains are inhomogeneously distributed with an increase in the presence of voids. From the SEM micrograph for $x = 0.7$ (*i.e.*,$0.3Ba_5TbTi_3V_7O_{30} - 0.7BiFeO_3$) the average size of the grain is about ~ 1.4μm having more angular and cubicle shape. As x increases, the size of the grain decreases along with a decrease in porosity. The distribution of microstructure suggests the presence of polycrystalline grain texture. From SEM micrograph for x =1 (*i.e.*, $BiFeO_3$). It can be seen that the process is more or less complete in the sintering process. It has become dense, and a few amounts of scattered pores are also present. There's also the presence of needle types of grains along the axis.

Scanning electron microscopy (SEM) is widely used in current material research. The main advantages of SEM are a large depth of focus and no limitation in the size and shape of the bulk specimens. The introduction of SEM significantly benefits the sintering process. An incomplete sinter specimen has complex and irregular surfaces, which need visual interpretation through the deep field. SEM provides a 3-D image and a clear image of the specimen.

7.3.3. Dielectric Study

Ferroelectric materials are considered to be important because of their properties like electro-optic, pyroelectric, piezoelectric, elastic-optic and electro-mechanical for which these materials apply to various electronic, electro-optic, computer and communication devices like memories, light modulator and deflector, frequency changer, microphones, filters and detectors. All these characteristics of ferroelectric composites are related to their response to electrical stimuli. Electrical behaviour is important for its applications. Ferroelectrics has properties of (1) High dielectric constant (500-4000) in comparison to other ins, hence useful for making energy storage and capacitors device, (2) Low tangent loss, (3) High resistivity (10^{11}-10^{13} Ωcm), (4) Moderate dielectric breakdown

strength & (5) Hysteresis (non-linear) electrical behaviour. Ferroelectric also has an optical and mechanical effect that interacts with electrical effects and produces electromechanical and electro-optical devices. Hence, electrical properties play a very important role in understanding and characterizing a ferroelectric material. Among various electrical properties, the dielectric study provides a vital role in providing information regarding ferroelectrics.

Dielectric properties of ferroelectrics over a wide temperature range are one of the key tools for understanding ferroelectricity in ceramics. In dielectric AC charge gets stored in both real (in-phase) and imaginary (out-phase) components causing either dielectric absorption or resistive leakage. The dielectric loss i.e., the ratio of the out-phase components to that of in-phase components is also called dissipation factor D (frequently expressed as the loss tangent).

$$tan\delta = \frac{\varepsilon''}{\varepsilon'} \qquad (7.2)$$

where, ε', $\varepsilon''$are real (in-phase) and imaginary (out-phase) components of complex dielectric constant $\epsilon^* = \epsilon' - i\,\epsilon''$

A dielectric constant measured in constant or zero stress is known as a free dielectric constant (ϵ). When it is measured at constant strain then is called clamp dielectric constant (ϵ_s). The free and clamp dielectric constant may differ from piezoelectric materials and is related via electromechanical coupling factor (K) i.e. $\epsilon_s = K(1 - \epsilon'')$, K could be as high as 0.7 or more for strong piezoelectric materials. For normal substances, the relative dielectric constant value is low, usually less than 5 for organic material and less than 20 for inorganic solids. Whereas ferroelectrics have high dielectric constant values having a range of hundreds to several thousand.

Ferroelectric has a crystal matrix consisting of pores and grains. Division of the surface matrix and grains or pores requires extra energy and, they influence physical properties like dielectric constant, tangent loss, Curie temperature, etc. Thermo-dynamical model of ferroelectric ceramics suggests some features as follows:

- Due to properties like micro-structure (density, dimension, pores, and grains), impurities, etc. there are changes in a phase transition.
- In the transition region, there is no sharp change in the dielectric constant value,
- Rather it is more of a round peak spread in a wide range of temperatures.
- Curie temperature (transition) is strongly dependent on the grains and pores and the micro-volume inhomogeneity in the ceramics.
- Curie-Weiss constant value of composites is higher than single crystal and it strongly depends on the dimension and pore density.
- Temperature of tan δ_{max} does not coincide with that of ϵ_{max} temperature in ceramics.

Figure 7.5 shows the frequency variation of the ε_r for (1-x)$Ba_5TbTi_3V_7O_{30}$-x$BiFeO_3$ at room temp, as frequency increases from 4Hz to 1kHz, the ε_r decreases for x =0 (i.e. $Ba_5TbTi_3V_7O_{30}$) from ~50 to ~17, for $x = 0.3$ (*i.e.*,$0.7Ba_5TbTi_3V_7O_{30} - 0.3BiFeO_3$) from ~ 30 to ~ 20, for x =0.5 (*i.e.*,$0.5Ba_5TbTi_3V_7O_{30} - 0.5BiFeO_3$) from ~35 to ~25 and for x =0.7(i.e.,$0.3Ba_5TbTi_3V_7O_{30} - 0.7BiFeO_3$) from ~45 to ~30, the observed trend (*i.e.*, as frequency increases dielectric constant should decrease) is as observed for typical dielectric materials. It is being found that as $BiFeO_3$ increases the dielectric constant value decreases.

Figure 7.6 shows the variation of tanδ (loss tangent) with frequency for (1-x)$Ba_5TbTi_3V_7O_{30}$-x$BiFeO_3$ at room temp. It can be seen that as frequency increases from 4Hz to 1kHz, tanδ (tangent loss) decreases for x=0 (i.e. $Ba_5TbTi_3V_7O_{30}$) from ~1.3 to ~0.15, for x=0.3 (i.e. 0.7$Ba_5TbTi_3V_7O_{30}$-0.3$BiFeO_3$) from ~0.35 to ~0.08, for x=0.5 (i.e. 0.5$Ba_5TbTi_3V_7O_{30}$-0.5$BiFeO_3$) from ~0.24 to ~0.03 and for x=0.7 (i.e. 0.3$Ba_5TbTi_3V_7O_{30}$-0.7$BiFeO_3$) from ~0.34 to ~0.05, the trend is observed for typical dielectric materials. As $BiFeO_3$ increases, the tangent loss value also increases because of the semiconducting nature of $BiFeO_3$.

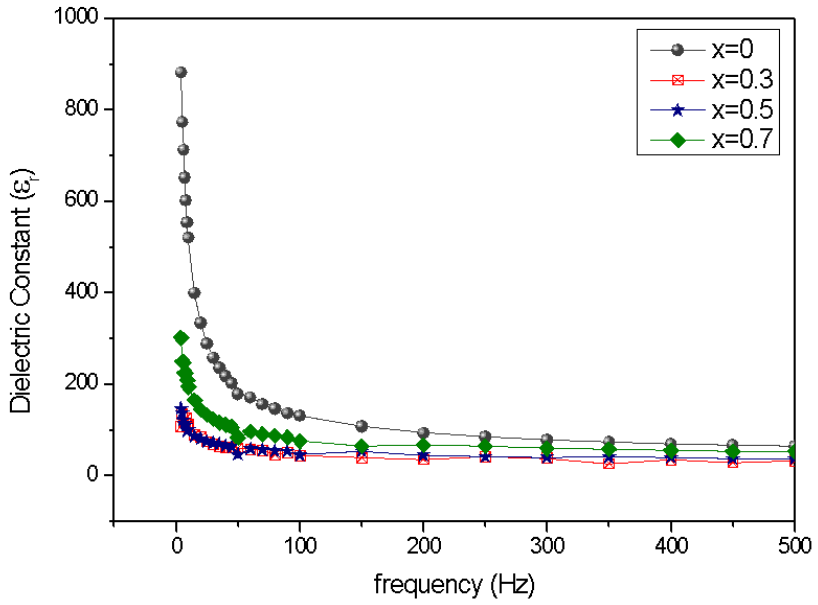

Figure 7.5. Frequency variation of ε_r for (1-x)$Ba_5TbTi_3V_7O_{30}$-x$BiFeO_3$ at room temp.

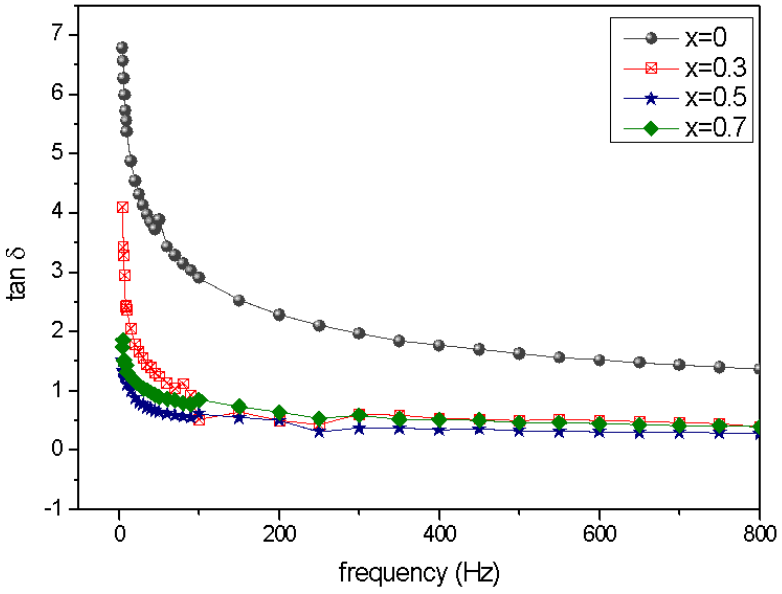

Figure7.6. Frequency variation of tanδ of (1-*x*)$Ba_5TbTi_3V_7O_{30}$-*x*$BiFeO_3$ at room temp.

Variation of ε (dielectric constant value) with temperature (room temperature to 500°C) for (1-x)$Ba_5TbTi_3V_7O_{30}$-x$BiFeO_3$ is shown in Figure 7.7 for the selected static frequency at 1kHz. With the rise in temperature dielectric constant (ε_r) also increases till it attains its peak value (at transition temperature T_C) after which it decreases. The presence of dielectric anomaly may be because of the long-range migration of dipole orientation and charge species. After a certain period above critical temperature T_C, the value of the dielectric constant keeps on increasing due to the establishment of space charge polarization at high temperatures From Table 7.1 It could be observed that for x=0 (i.e. $Ba_5TbTi_3V_7O_{30}$) the dielectric constant value (ε_{max}) is ~1090 and with the addition of $BiFeO_3$ the maximum dielectric constant reduces to 550 for x=0.3 (i.e. 0.7$Ba_5TbTi_3V_7O_{30}$-0.3$BiFeO_3$) and for x=0.5 (i.e. 0.5$Ba_5TbTi_3V_7O_{30}$-0.5$BiFeO_3$) it reduces to ~ 630 whereas for x=0.7 (i.e. 0.3$Ba_5TbTi_3V_7O_{30}$-0.7$BiFeO_3$) it reduces to 470. At room temperature, the maximum values of the dielectric constant of any of the composites are less than the dielectric constant (ε_{RT} ~ 670) of the pure ferroelectric.

Thus, it could be concluded that the dielectric characteristics of $BiFeO_3$ are improved when it is mixed with ferroelectric i.e., $Ba_5TbTi_3V_7O_{30}$.

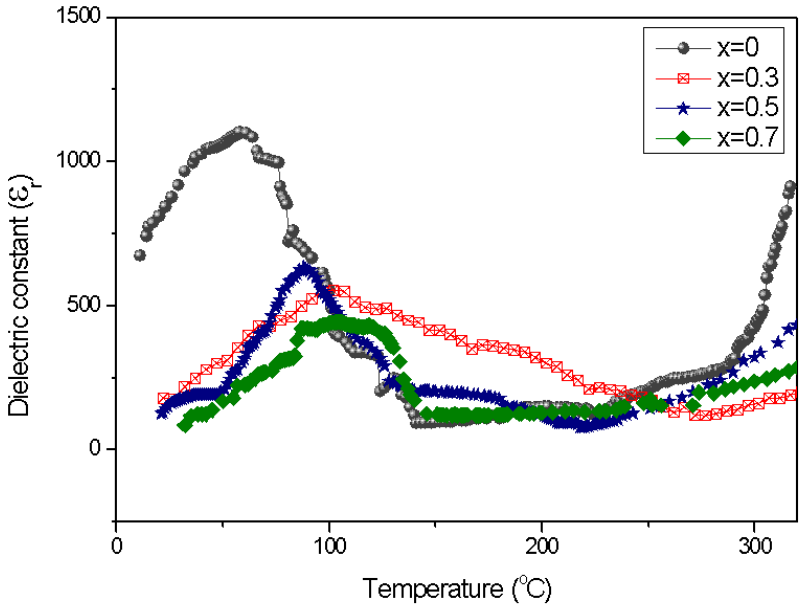

Figure 7.7 Variation of ε_r with temperature for (1-x)$Ba_5TbTi_3V_7O_{30}$-x$BiFeO_3$ at 1kHz.

Variation of tan δ (loss tangent) with a temp for (1-x)$Ba_5TbTi_3V_7O_{30}$-x$BiFeO_3$ at 1000Hz about the temperature range (RT- 500℃) can be seen in Figure 7.8. It is being observed that with an increase of $BiFeO_3$ in the solid solution tangent loss (tan δ) also increases which may be because of the semiconducting nature of $BiFeO_3$ leading to increased tangent loss. As $BiFeO_3$ content further increases the value of loss tangent (tan δ) also increases. For x = 0.3, the tangent loss is 4.35 and the tangent loss is maximum for x=0.5 i.e., 6.75. However, there is an anomaly i.e., for x=0.7 tangent loss is 3.65 i.e., moderate tangent loss in comparison to its neighbour indicating that the tangent loss is strongly dependent on the crystal structure.

The value of tanδ is very large at high temperatures, which is due to conductivity enhancement because of the addition of $BiFeO_3$, which might cause the decline of ferroelectric domain walls.

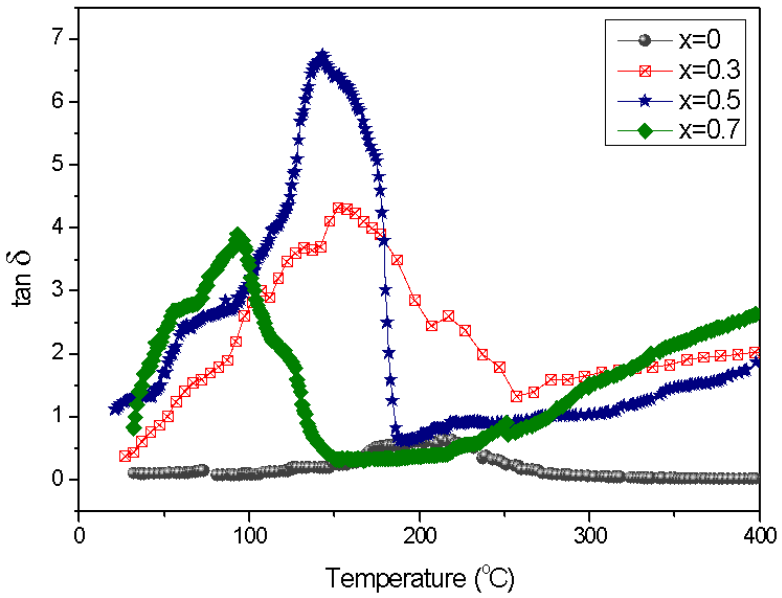

Figure 7.8. Variation of tanδ with temperature for (1-x)$Ba_5TbTi_3V_7O_{30}$-x$BiFeO_3$ at 1kHz.

Table 7.1. Dielectric properties like dielectric constant and loss tangent of (1-x)$Ba_5TbTi_3V_7O_{30}$-x$BiFeO_3$ at 1kHz.

Samples	ε_{RT}	ε_{max}	tan δ_{RT}	tan δ_{max}	Transition Temp
x= 0.7	84	470	0.796	3.65	105
x= 0.5	157	630	1.232	6.75	88
x=0.3	172	550	0.52	4.35	103
x= 0.0	671	1090	0.133	0.610	83

7.3.4 Electrical Conductivity

Electrical conduction in the dielectric matter is due to the movement of weakly bound charge particles in the presence of an external electric field. It is mostly found in polycrystalline and amorphous materials. Conduction is measured via a parameter called electrical conductivity. The study of electrical conductivity plays an important role in the physics of ferroelectrics. Solids are categorized as primarily ionic or electronic conductors depending upon which of the charge carrier is predominant i.e.

electrons/holes or cations/ions. Non-linear dielectric and ferroelectric crystals in general show ionic conduction. Electric polarization is pronounced in crystals that have oxygen octahedra like Barium Titanate ($BaTiO_3$) ferroelectrics which may be because of oxygen defects/vacancy in the crystal structure. Whereas, in the case of ionic crystals under an electric field the phenomenon of electrical conduction is because of the movement of the crystal lattice's host ions and such kind of conduction is called intrinsic conduction which mostly appears at high temperatures. These ions mostly cause electrical conduction in ionic crystals. Which also contain impurity ions and are located at the defect site. These ions give rise to extrinsic or impurity conduction with high conductivity and low activation energy. In real crystals, the electrical conductivity is mainly intrinsic whereas in low temperatures it is extrinsic in nature. The variation in conductivity (σ) with temperature could be described as:

$$\sigma = A_1 e^{\frac{-E_g}{kT}} + A_2 e^{\frac{-E_x}{kT}} \qquad (7.3)$$

where E_g and E_x are activations energy of intrinsic band gap and extrinsic impurity level conduction. In some cases, electrical conductivity is also associated with impurities. Through a literature survey, it was found that the conduction increases sharply when rare earth ions are introduced into TB niobates.

Figure 7.9 shows the Variation of AC conductivity ($\ln\sigma$) with the inverse of temperature (1/T) at constant frequency 1kHz for the composite $(1-x)Ba_5TbTi_3V_7O_{30} - xBiFeO_3$ for different x values. Due to dielectric phase transition characteristics, abnormality in conductivity is observed in the graph nearly at a similar position as their respective Curie temp.

For $Ba_5TbTi_3V_7O_{30}$ i.e.x=0, the graph is distributed in three different regions having different slopes representing two paraelectric regions termed as (II, III)along with one ferroelectric region as I. Variation of σ_{ac}in various temperature range indicates the presence of thermally activate process which is because of the incidence of immobile species at lower temperature and defects at high temperature. A low activation energy value indicates that to activate the electrons/carriers for conduction a small energy is required. A similar kind of trend of ac conductivity was observed in similar materials [52]. For $0.7Ba_5TbTi_3V_7O_{30} - 0.3BiFeO_3$ *i.e.*, x= 0.3 the graph is distributed into three different regions with two ferroelectric regions (I, II) and one paraelectric region III categorised by three different slopes. Conductivity is high at a higher temperature which is a common characteristic for most dielectric materials The main contributor to conductivity in region III may be space charge. For $0.5Ba_5TbTi_3V_7O_{30} - 0.5BiFeO_3$ *i.e.*, x= 0.5, the graph is distributed into four different regions with two ferroelectric regions (I, II) and two paraelectric regions (III, IV). Slope variation at different temperatures indicates different mechanisms of conduction and hence has different activation energies. For $0.3Ba_5TbTi_3V_7O_{30} - 0.7BiFeO_3$ *i.e.*, $x = 0.7$, the graph is distributed into three different regions with two ferroelectric regions (I, II) and one paraelectric region III categorized by different slopes having different activation energies.

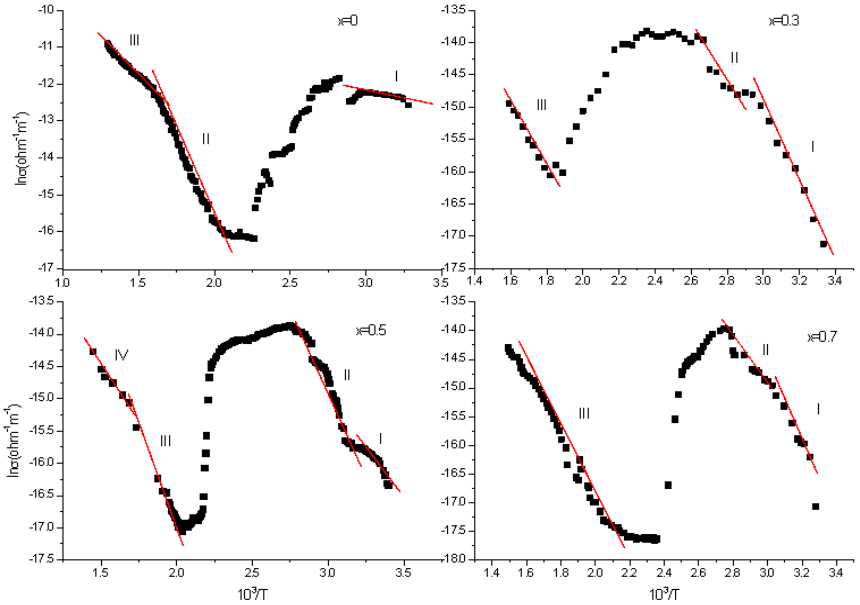

Figure 7.9. $\ln \sigma_{ac}$v/s $10^3/T$for$(1-x)\mathrm{Ba_5TbTi_3V_7O_{30}} - x\mathrm{BiFeO_3}$ at 1kHz.

Using the Arrhenius equation values of activation energy (E_a) is measured at different regions and summarized in Table 7.2. Conductivity is higher at high temperatures as per the characteristics of most dielectric materials [52, 53]. The variation of AC conductivity (σ_{ac}) in a given temperature range indicate thermally activated transport properties which may be because of immobile species at lower temperature and the existence of defects at high temperature. It can be inferred that to activate electrical conduction by the charge carriers only a small amount of energy is needed. Such a trend was also observed for materials of similar kinds [53].

Table 7.2 Activation energy (E_A) of $(1-x)\mathrm{Ba_5TbTi_3V_7O_{30}} - x\mathrm{BiFeO_3}$ at 1kHz.

Compounds	E_A (eV)			
	I	II	IIII	IV
x=0.0	0.05	0.713	0.337	--
x=0.3	0.472	0.341	0.434	--
x=0.5	0.193	0.476	0.451	0.315
x=0.7	0.629	0.308	0.421	--

The occurrence of different types of conduction mechanisms corresponding to different activation energy values is indicated by different slopes in the graph ($\ln\sigma$ vs 10^3/T). Variation of σ_{ac} over a given temperature range suggests that the transport properties are thermally activated which obeys Arrhenius behaviour. At the vicinity of Curie temperature, the conductivity is being observed which may be of order-disorder type

resulting from the rearrangement of lattices during the Ferro-paraelectric phase transition. An increase in activation energy may be because of the hopping of the charging mechanism associated with the oxidation-reduction route.

The graphs show that as temperature increases, AC conductivity also increases showing NTCR (negative temperature coefficient of resistance) which is a characteristic behaviour of ferroelectric materials.

7.4. CONCLUSION

In $Ba_5TbTi_3V_7O_{30}$, when $BiFeO_3$is added the value dielectric constant reduces and simultaneously the tangent loss increases. This may be because of mixing of different phases may result in the modification of the morphotropic phase boundary. As, $BiFeO_3$ is further increased in solid solution the value of dielectric constant decreases along with more increase of tangent loss. It may be because $BiFeO_3$ is semiconducting in character resulting in an electrical conduction increase.

There is also an increase in activation energy as $BiFeO_3$ in solid solution increases. The ac conductivity graph shows that as temperature increases there is also an increase in associated conductivity values hence showing a negative temperature coefficient of resistance (NTCR) identical to that of semiconductors. Thus, with the effect of $Ba_5TbTi_3V_7O_{30}$the ferroelectric property of $BiFeO_3$ is improved.

7.5. REFERENCES

[1] J. Valasek, Dielectric anomalies in Rochelle salt crystals, Phys. Rev., 24(5) (1924) 560. https://doi.org/10.1103/PhysRev.24.560

[2] J.C. Burfoot, and G W. Taylor, Polar dielectrics and their applications. Univ of California Press, 2022.

[3] S.S. Rajput, R. Katoch, K.K. Sahoo, G.N. Sharma, S.K. Singh, R. Gupta, and A. Garg, Enhanced electrical insulation and ferroelectricity in La and Ni co-doped $BiFeO_3$ thin films. J. Alloys Comp., 621 (2015) 339-344. https://doi.org/10.1016/j.jallcom.2014.09.161

[4] S.P. Muduli, S. Parida, S.K. Behura, S. Rajput, S.K. Rout, S. Sareen, Synergistic effect of graphene on the dielectric and piezoelectric characteristic of PVDF-(BZT-BCT) composite for energy harvesting applications, Polym. Adv. Technol., 33 (2022) 3628-3642. https://doi.org/10.1002/pat.5816

[5] S.S. Rajput, S. Keshri, Structural and microwave properties of (Mg,Zn/Co)TiO_3 dielectric ceramics. J. Mater. Eng. Perform., 23 (2014) 2103-2109. https://doi.org/10.1007/s11665-014-0950-7

[6] J. F. Nye, Some geometrical relations in dislocated crystals. Acta Metallurgica, 1(2) (1953) 153-162. https://doi.org/10.1016/0001-6160(53)90054-6

[7] W. A. Wooster, Crystal symmetry and physical properties by S. Bhagavantam, Acta Crystallographica., 21(6) (1966) 1016-1016. https://doi.org/10.1107/S0365110X66004481

[8] M. E. Lines, A. M. Glass and Gerald Burns, Principles and Applications of Ferroelectrics and Related Materials, Physics Today., 31(9) (1978) 56. https://doi.org/10.1063/1.2995188

[9] B. M.Tareev, Physics of dielectric materials, Mir publishers, 1975.

[10] G. Busch, How I discovered the ferroelectric properties of KH_2PO_4, Ferroelectrics, 71 (1987) 43-47. https://doi.org/10.1080/00150198708224828

[11] W. Känzig, Ferroelectrics and antiferroeletrics. Solid State Physics, 4. Academic Press, 1957, 1-197. https://doi.org/10.1016/S0081-1947(08)60154-X

[12] J. Wang, J. B. Neaton, H. Zheng, V. Nagarajan, S. B. Ogale, B. Liu, D. Viehland, M. Wuttig, R. Ramesh, Epitaxial $BiFeO_3$ multiferroic thin film Heterostructures, Science, 299(5613) (2003) 1719-1722. https://doi: 10.1126/science.1080615

[13] M. Kumar, K. L. Yadav, and G. D. Varma, Large magnetization and weak polarization in sol–gel derived $BiFeO_3$ ceramics, Materials Letters, 62 (8-9) (2008) 1159-1161. https://doi.org/10.1016/j.matlet.2007.07.075

[14] N. A. Hill, P. Bättig, and C. Daul. First principles search for multiferroism in $BiCrO_3$, The Journal of Physical Chemistry B, 106(13) (2002) 3383-3388. https://doi.org/10.1021/jp000114x

[15] M. Fiebig, Revival of the magnetoelectric effect, Journal of physics D: applied physics, 38(8) (2005) R123. https://doi.org/10.1088/0022-3727/38/8/R01

[16] C. T. Munoz, J. P. Rivera, A. Bezinges, A. Monnier, and H. Schmid, Measurement of the quadratic magnetoelectric effect on single crystalline $BiFeO_3$. Jpn. J. Appl Phy. 24 (1985) 1051–1053. https://doi.org/10.7567/JJAPS.24S2.1051

[17] J. R. Teague, R. Gerson, and W. J. James, Dielectric hysteresis in single crystal $BiFeO_3$, Solid State Communications, 8(13) (1970) 1073-1074. https://doi.org/10.1016/0038-1098(70)90262-0

[18] P. Fischer, M. Polomska, I. Sosnowska, and M. Szymanski, Temperature dependence of the crystal and magnetic structures of $BiFeO_3$, Journal of Physics C: Solid State Physics, 13(10) (1980) 1931-1940. https://doi:10.1088/0022-3719/13/10/012

[19] G. A. Smolenskiĭ, N. N. Kraĭnik, Progress in ferroelectricity, Soviet Physics Uspekhi, 12 (1969) 271. https://doi.org/10.1070/PU1969v012n02ABEH003937

[20] R. T. Smith, G. D. Achenbach, R. Gerson, and W.J. James, Dielectric properties of solid solutions of $BiFeO_3$ with $Pb(Ti,Zr)O_3$ at high temperature and high frequency, J. Appl. Phys., 39(1) (1968) 70-74. https://doi.org/10.1063/1.1655783

[21] M. M. Kumar, A. Srinivas, G. S. Kumar, and S. V. Suryanarayana, Investigation of the magnetoelectric effect in BiFeO3-BaTiO3 solid solutions, Journal of Physics: Condensed Matter., 11(41) (1999) 8131. https://doi.org/10.1088/0953-8984/11/41/315

[22] M.M. Kumar, A. Srinivas, S. V. Suryanarayanan, and T. Bhimasankaram Dielectric and impedance studies on $BiFeO_3$–$BaTiO_3$ solid solutions, physica status solidi (a), 165(1) (1998) 317-326. https://doi.org/10.1002/(SICI)1521-396X(199801)165:1<317::AID-PSSA317>3.0.CO;2-Y

[23] M. M. Kumar, A. Srinivas, and S. V. Suryanarayana, Structure property relations in $BiFeO_3$/$BaTiO_3$ solid solutions, J. Appl. Phys., 87(2) (2000) 855-862. https://doi.org/10.1063/1.371953

[24] W. M. Zhu, H. Y. Guo, and Z. G. Ye, Structure and properties of multiferroic $(1-x)BiFeO_3$–$xPbTiO_3$ single crystals, J. Mater. Res., 22(8) (2007) 2136-2143. https://doi.org/10.1557/jmr.2007.0268

[25] W. M. Zhu, H-Y. Guo, and Z. G. Ye, Structural and magnetic characterization of multiferroic $(BiFeO_3)_{1-x}(PbTiO_3)_x$ solid solutions, Phys. Rev. B, 78(1) (2008) 014401. https://doi.org/10.1103/PhysRevB.78.014401

[26] K. S. Nalwa, A. Garg, and A. Upadhyaya, Effect of samarium doping on the properties of solid-state synthesized multiferroic bismuth ferrite, Mater. Lett., 62(6-7) (2008) 878-881. https://doi.org/10.1016/j.matlet.2007.07.002

[27] S. Chandarak, A. Ngamjarurojana, S. Srilomsak, P.Laoratanakul, S. Rujirawat, and R. Yimnirun, Dielectric properties of $BaTiO_3$-modified $BiFeO_3$ ceramics, Ferroelectrics, 410(1) (2010) 75-81. https://doi.org/10.1080/00150193.2010.492724

[28] S. Rajput, X. Ke, X. Hu, M. Fang, D. Hu, F. Ye, X. Ren, Critical triple point as the origin of giant piezoelectricity in $PbMg_{1/3}Nb_{2/3}O_3$-$PbTiO_3$ system. J. Appl. Phys., 128 (2020) 104105. https://doi.org/10.1063/5.0021765

[29] Sonika, S.K. Verma, S. Samanta, A.K. Srivastava, S. Biswas, R.M. Alsharabi, S. Rajput, Conducting Polymer Nanocomposite for Energy Storage and Energy Harvesting Systems. Adv. Mater. Sci. Eng., 2022 (2022) 1-23. https://doi.org/10.1155/2022/2266899

[30] B. A. Scott, E. A. Giess, G. Burns, and D. F. O'kane, Alkali-rare earth niobates with the tungsten bronze-type structure, Materials Research Bulletin. 3(10), (1968) 831-842. https://doi.org/10.1016/0025-5408(68)90100-1

[31] M. Fang, S. Rajput, Z. Dai, Y. Ji, Y. Hao, X. Ren, Understanding the mechanism of thermal-stable high-performance piezoelectricity. Acta Materialia, 169, (2019) 155-161. https://doi.org/10.1016/j.actamat.2019.03.011

[32] J. E. Geusic, H. J. Levinstein, J. J. Rubin, S. Singh, and L. G. Van Uitert, The nonlinear optical properties of $Ba_2NaNb_5O_{15}$, Applied Physics Letters, 11(9) (1967) 269-271. https://doi.org/10.1063/1.1755129

[33] K. S. Singh, R. Sati, and R. N. P. Choudhary, X-ray, scanning electron microscopic and dielectric properties of ferroelectric $Ba_2Na_3RNb_{10}O_{30}$ (R= La or Sm) ceramics, J. Mater. Sci. Lett., 11(11) (1992) 788-790. https://doi:10.1007/BF00729494

[34] A. Panigrahi, N. K. Singh, and R. N. P. Choudhary, Structural and electrical properties of Ba5RTi3Nb7O30 [R= Eu, Gd] ceramics, J. Mater. Sci. Lett., 18(19) (1999) 1579-1581. https://doi.org/10.1023/A:1006656115028

[35] A. Panigrahi, N. K. Singh, and R. N. P. Choudhary, Diffuse phase transition in $Ba_5NdTi_{3-x}Zr_xNb_7O_{30}$ ferroelectric ceramics, Journal of Physics and Chemistry of Solids, 63(2) (2002) 213-219. https://doi.org/10.1016/S0022-3697(01)00132-9

[36] Y. Wu, C. Nguyen, S. Seraji, M. J. Forbess, S. J. Limmer, T. Chou, & G. Cao, Processing and properties of strontium bismuth vanadate niobate ferroelectric ceramics. J. Amer. Ceram. Soc., 84(12) (2001) 2882-2888. https://doi.org/10.1111/j.1151-2916.2001.tb01109.x

[37] M. H. Francombe and B. Lewis, Structural, dielectric and optical properties of ferroelectric lead metaniobate, Acta Crystallographica. 11(10) (1958) 696-703. https://doi:10.1107/S0365110X58001882

[38] M. H. Francombe, The relation between structure and ferroelectricity in lead barium and barium strontium niobates, Acta Crystallographica. 13(2) (1960) 131-140. https://doi.org/10.1107/S0365110X60000285

[39] E. C. Subbarao, and G. Shirane, Nonstoichiometry and Ferroelectric Properties of PbNb2O6-Type Compounds, The Journal of Chemical Physics. 32(6) (1960) 1846-1851.https://doi.org/10.1063/1.1731032.

[40] E. A. Giess, B. A. Scott, G. Burns, D. F. O'kane, and A. Segmüller, Alkali Strontium-Barium-Lead Niobate Systems with a Tungsten Bronze Structure: Crystallographic Properties and Curie Points, Journal of the American Ceramic Society. 52(5) (1969) 276-281. https://doi.org/10.1111/j.1151-2916.1969.tb09183.x

[41] A. A. Ballman and H. Brown, The growth and properties of strontium barium metaniobate, $Sr_{1-x}Ba_xNb_2O_6$, a tungsten bronze ferroelectric, J. Crystal Growth., 1(5) (1967) 311-314. https://doi.org/10.1016/0022-0248(67)90038-3

[42] T. Badapanda, R. Harichandan, T. B. Kumar, S. Parida, S.S. Rajput, P. Mohapatra, R. Ranjan, Improvement in dielectric and ferroelectric property of dysprosium doped barium bismuth titanate ceramic, J. Mater. Sci.: Mater. Electron., 27 (2016) 7211-7221. https://doi.org/10.1007/s10854-016-4686-z

[43] K. Kathayat, A. Panigrahi, A. Pandey, and S. Kar, Effect of Holmium doping in $Ba_5RTi_3V_7O_{30}$ (R= rare earth element) compound, Integrated Ferroelectrics., 118(1) (2010) 8-15. https://doi.org/10.1080/10584587.2010.489461

[44] H. Doley, P.K. Swain, A. Panigrahi, and G.T. Tado, Structural and ferroelectric properties in the solid solution (Ba5TbTi3V7O30) x(BiFeO3)1-x

Ferroelectrics, 568(1) (2020) 104-111. https://doi.org/10.1080/00150193.2020.1811034

[45] H. Doley, P.K. Swain, A. Panigrahi, and G.T. Tado, Study of structural and ferroelectric properties of the composite $Ba_5RTi_3V_7O_{30}$ (R= Pr, Tb), Bull. Pure Appl. Sci. Phys. D, 38 (2019) 65-72 doi: 10.5958/2320-3218.2019.00011.3

[46] A. Magnéli, The crystal structure of tetragonal potassium tungsten bronze, Arkiv for Kemi., 1(3) (1949): 213-221.

[47] R. R. Neurgaonkar, J. G. Nelson, J. R. Oliver, and L. E. Cross, Ferroelectric and structural properties of the tungsten bronze system K_2Ln3+ Nb5O15, Ln= La to Lu, Mater. Res. Bull., 25(8) (1990) 959-970. https://doi.org/10.1016/0025-5408(90)90002-J

[48] P. B. Jamieson, S. C. Abrahams, and J. L. Bernstein, Ferroelectric tungsten bronze-type crystal structures. I. Barium Strontium niobate $Ba_{0.27}Sr_{0.75}Nb_2O_5$, J. Chem. Phys., 48(11) (1968) 5048-5057. https://doi.org/10.1063/1.1668176

[49] A. Srinivas, D. W. Kim, K. S. Hong & S. V. Suryanarayana, Observation of ferroelectromagnetic nature in rare-earth- substituted bismuth iron titanate, Appl. Phys. Lett., 83(11) (2003) 2217-2219. https://doi.org/10.1063/1.1610255

[50] A. Srinivas, F. Boey, T. Sritharan, D.W. Kim, & K.S. Hong, Processing and study of dielectric and ferroelectric nature of $BiFeO_3$ modified SrBi2Nb2O9, Ceram. Int., 30(7) (2004) 1427-1430. https://doi.org/10.1016/j.ceramint.2003.12.080

[51] Y. Li, M. Liu, J. Gong, Y. Chen, Z. Tang, & Z. Zhang, Grain-boundary effect in zirconia stabilized with yttria and calcia by electrical Measurements, Mater. Sci. Eng. B., 103(2) (2003) 108-114. https://doi.org/10.1016/S0921-5107(03)00162-4

[52] X. Hu, S. Rajput, S. Parida, J. Li, W. Wang, L. Zhao, X. Ren, Electrostrain Enhancement at Tricritical Point for $BaTi_{1-x}Hf_xO_3$ Ceramics. J. Mater. Eng. Perform., 29 (2020) 5388-5394. https://doi.org/10.1007/s11665-020-05003-5

[53] K.S. Rao, T. N. V. K. V. Prasad, A. S. V. Subrahmanyam, J. H. Lee, J. J. Kim, & S. H. Cho, Dielectric and pyroelectric properties of BSNN ceramics: effect of Ba/Sr ratio and La_2O_3 addition, Mater. Sci. Eng. B., 98(3) (2003) 279-285. https://doi.org/10.1016/S0921-5107(03)00064-3